Groundwater nitrate and fluoride profiles, sources, and health risk assessment in the coal mining areas of Salt Range, Punjab Pakistan

Noshin Masood[a], Karen A. Hudson-Edwards[b], Abida Farooqi[a*]

[a] Environmental Geochemistry Laboratory, Department of Environmental Sciences, Faculty of Biological Sciences, Quaid-i-Azam University, Islamabad, PO 45320, Pakistan

[b] Environment & Sustainability Institute and Camborne School of Mines, University of Exeter, Penryn, TR10 9EZ, UK

Correspondence to: Abida Farooqi, afarooqi@qau.edu.pk

Abstract

To assess the loading profiles of groundwater nitrate (NO_3^-) and fluoride (F^-), spatial distributions, geochemistry and associated health risks were determined for 131 groundwater samples from Eastern (ESR), Central (CSR) and Trans-Indus Salt Ranges (TSR) in Pakistan. Groundwater NO_3^- concentrations were 0.2-308 mg/L (mean 59 mg/L) in ESR, 2.7-203 mg/L (mean 73 mg/L) in CSR and 1.1-259 mg/L (mean 69 mg/L) in the TSR. Forty-one %, 57 %, and 36% of the ESR, CSR and TSR samples, respectively, exceeded the WHO and Pak-NEQs permissible limit of 50 mg/L NO_3^-. Likewise, groundwater F^- concentrations ranged from 0.1-1.8 mg/L (mean 0.6 mg/L), 0.1-2.7 mg/L (mean 0.9 mg/L) and 0.3-2.5 mg/L (mean 1.6 mg/L) mg/L in the ESR, CSR, and TSR sites, respectively. In this case, 3 %, 17 %, and 27% of the ESR, CSR, and TSR samples, respectively, exceeded the WHO and Pak-NEQs permissible limit of 1.5 mg/L F. Oxidation of coal and coal waste resulted in release of NO_3^- to groundwater. By contrast, enrichment of F^- in groundwater was due to dissolution and cation exchange processes. Elevated values of the Higher Pollution Index (PI) and Health Risk Index (HRI) reflect a non-acceptable carcinogenic risk for drinking water NO_3^- and F^- which should be addressed at priority basis in order to protect human health.

Key Words: groundwater; nitrate; fluoride; geochemistry; drinking water; health risk assessment

1. Introduction

Coal is an important source of fuel in many countries, but its use can release CO_2, generate acid mine drainage, and release metal and metalloid contaminants (Sadasivam et al. 2019). Among these contaminants, NO_3^- and F^- are relatively unrecognized hazards in coal-based aquifers (Rezaei et al. 2017). People living in coal mining areas are vulnerable to these potentially toxic elements. Since 1970, NO_3^- contamination has been a globally recognized phenomenon that can lead to water contamination, safe drinking water supply complications and spread of nitrogen-regulated pathogenic and carcinogenic diseases (Katz et al. 2004; Rivett et al. 2007; Roy et al. 2007; Stuart et al. 2011; Stone and Edmunds 2014). Nitrate is non-toxic to humans, but upon reduction in the gastrointestinal tract, its by-product nitrite can cause carcinogenic (including gastric, stomach, esophageal cancers) as well as neurogenic impacts of newborns such as methemoglobinemia (Ward et al. 2005; Ako et al. 2014). Nitrate is the oxidized product of elemental nitrogen (N), ammonium (NH_4^+), and nitrite (NO_2^-) ions. Being an extremely stable species of nitrogen upon moving through water or soil bodies, it does not form complexes and/or insoluble compounds (Tew 2018). Therefore, percolation of NO_3^- into the aquatic environment can contaminate both surface and groundwater.

Various practices and processes during coal mining unlock this fixed nitrogen and release it into environment in the form of NO_3^-, nitrite, or ammonia (Hendry et al. 2018). For example, the elemental nitrogen locked in the host coals upon excavation via nitrification and denitrification dissociates into NO_3^-, which can dissolve in surrounding soil and water (Bailey et al. 2013; Zaitsev et al. 2008; Mahmood et al. 2017; Villeneuve et al. 2017). In addition to this, during blasting, in coal mine spillages or during incomplete detonation and successive dissolution of explosives (a

mixture of ammonium nitrate and fuel oil, ANFO, Bailey et al. 2013), or gunpowder in oxidizing conditions high amounts of NO_3^- can be released to the host environment (Mahmood et al. 2017; Villeneuve et al. 2017).

Continuous mining practices leading to deformation, strata movement, and subsidence. These can alter the physical properties of soils and result in their nitrogen leaching into soils as nitrate (Kuter et al. 2014; Masilionytė et al. 2014; Endale et al. 2017). Such increasing trend of NO_3^- levels in coal mining areas have been demonstrated in Elk Valley and West Line Creek, Canada, where rising concentrations (from 6.5 mg/l in 1994 to 38.5 mg/l NO_3^- in 2006) were correlated to increasing volumes of coal mine waste rock (Mahmood et al. 2017; Hendry et al. 2018). Such environmental impacts could lead to nutrient imbalances in aquatic systems that in turn could lead to eutrophication (Jahangir et al. 2012). Due to the negative health impacts of ingesting NO_3^- from drinking water, the World Health Organization (WHO) has recommended groundwater maximum permissible concentrations of 50 mg/l for NO_3^- and 10 mg/l for NO_3 -N (WHO 2011). Excessive groundwater NO_3^- loading is a persistent problem, which requires effective management and a complete understanding of its source and chemical transport mechanisms. To develop management strategies, groundwater characteristics have been studied to establish hydrogeological settings. Studies have been conducted to evaluate fertilizers as a source for drinking water NO_3^- contamination (Daud et al. 2017; Chen et al. 2017; Shukla and Saxena 2018), but the role of coal and coal mining practices as a nitrate source to groundwater is less well understood.

Fluoride (F^-) is another potentially toxic chemical that can negatively impact on drinking water associated with coals derived from mineral matter such as fluorapatite and fluorspar minerals (Wu et al. 2004). Fluoride can form soluble complexes with metal and nonmetal ions such as Fe^{3+}, Al^{3+}, Mg^{2+}, Na^+, Ca^{2+} and H^+ (Li et al. 2016). Fluorine concentrations in coals generally range between

100 and 300 mg/kg. The fluorine is closely related to the coal sulfur and also shows strong non-polar affinity for aluminosilicate minerals (Guohua et al. 2019). For instance, kaolinite and muscovite are the primary carriers of F- in coal (Xiong et al. 2017). Oxidation of pyrite and weathering of aluminosilicate minerals during coal mining activities can cause release of F^- to soils and groundwater. The WHO and Pakistan National Environmental Quality Standards (PAK NEQs) recommended limit for drinking water F^- is 1.5 mg/L (Parvaiz et al. 2020). Although fluorine in minute concentrations is an essential element to human brains, higher doses can cause dental, skeletal and non-skeletal fluorosis (Rezaei et al. 2017; Younas et al. 2019). Atmospheric fluorine produced by coal combustion is the largest anthropogenic source of fluorine contamination in the USA (Wu et al. 2004). In addition, around 18,138,780 cases of dental and 1,594,799 cases of skeletal fluorosis were also reported in coal mining areas of China (Wu et al. 2004). In a study of the Zarand coal fields in Iran, coal mining industries and groundwater accelerated fluoride contamination and prevalence of dental fluorosis showed a strong relationship (Derakhshani et al. 2020). Due to such serious health impacts fluorine is considered among the top 10 most concerning chemicals for public health (Malek Mohammadi et al. 2017). Although the industrial impact of coal-based fluoride emissions and their health impacts have been studied in many areas, the relationship of coal mining and its associated groundwater fluoride contamination have been much less considered.

To fill the research gaps outlined above, this study was designed to determine the contribution of coal mining activities on groundwater NO_3^- and F^- contamination, enrichment patterns and geochemistry, and their potential health risk to humans. These results can provide the basis for policy implementations and for local ecological impacts and water management.

2. Materials and Methods

2.1 *Sampling and analysis*

The Salt Range coal mines are situated in the hills and low mountains that extend between the valleys of the Indus and Jhelum Rivers of Northern Punjab, Pakistan (Fig. 1). These mountains mostly comprise dolomite, sandstone, limestone, shale, gypsum, pyrite, and coal. Major coal reserves are concentrated in the Eastern, Central and Trans-Indus Salt Ranges. The Eastern and Central parts have semi-arid subtropical climatic conditions with average annual rainfall of 300-800 mm, whereas the Trans-Indus Salt Range has an arid climate and average annual rainfall of about 385 mm. To understand the potential impact of coal mining on NO_3^- and F^- loading, 131 groundwater samples from both shallow ($\leq$60 m) and deep (>60 m) depths were collected from preexisting wells across mining areas of the Salt Range: the Eastern Salt Range (ESR), Central Salt Range (CSR) and Trans-Indus Salt Range (TSR) (Makarwal) (Fig. 1). After filtration using 0.45 µm filter papers, pH, TDS, and electrical conductivity (EC) were measured *in situ* using a HANNA portable multi element meter. At each site, two pair of samples were taken. One pair was acidified using concentrated HNO_3 for cation analysis the other was not acidified and was used to analyze NO_3^- and F^-, SO_4^{2-} and Cl^-. All samples were taken in prewashed polyethylene stoppered plastic bottles, stored at 4 °C and transported to the Environmental Hydro-geochemistry Lab, Quaid-i-Azam University Islamabad. Nitrate concentrations were measured using a UV visible spectrophotometer (T80+ UV/Visible spectrophotometer), and F^-, SO_4^{2-} and Cl^- concentrations were determined using ion chromatography (Thermo Dual Channel ICS-5000+Ion Chromatography System) at the University of Leeds. Major cations were analyzed by Atomic Absorption Spectroscopy (Agilent 55AA) in the Environmental Hydro-geochemistry Lab, Quaid-

i-Azam University, Islamabad, following the methods defined by the American Public Health Association (APHA 2005). Data on well depth were collected through interviews with residents. In addition, coals of selected mines in the ESR, CSR and TSR sites were also analyzed for their mineralogical signatures by X-ray diffraction (XRD) technology (Phillips PW 1710 diffractometer technique using CuKα radiation).

2.2 *Risk Assessment*

The potential of a contaminant to cause risk can be assessed using a parameter known as the Pollution Index (PI). This is calculated as the concentration of a particular contaminant divided by the baseline concentration (standard) for that contaminant (EQ 1; (Bodrud-Doza et al. 2016; Nephalama and Muzerengi 2016).

$$Pollution\ index\ (PI) = \frac{Concentration\ of\ contaminant\ \left(\frac{mg}{L}\right)}{Baseline\ Standard\ \left(\frac{mg}{L}\right)} \quad \text{(EQ 1)}$$

In this study WHO standards for drinking water quality parameters were used as the baseline standards. A calculated PI of <1 indicates no pollution, and PI= >1 represents a significant degree of pollution.

2.3 Human Health Risk based on Exposure Assessment

The human health risk of adults, children, and infants were determined using exposure assessment. The Health Risk Index (HRI), based on the estimated daily intake (EDI), was calculated to evaluate the potential of these contaminants to cause carcinogenic health risks after ingestion (EQ 2, 3) (Ravindra and Mor 2019):

$$EDI = \frac{Cf \times Cd}{BW} \quad \text{(Eq 2)}$$

where C_f is the groundwater NO_3^- or F^- concentration in mg/L. C_d represents a daily average ingestion rate (i.e. 2 L/day for adults, 1.7 for children and 0.7 L/day is for infants), and BW is body weight (70 kg for adults, 30 kg for children and 4.9 kg for infants). Consumption pattern and body weight data used for the EDI calculations were generated through interviews of the local population of the study areas.

The HRIs for NO_3^- and F^- (HQ) were calculated using the following equation:

$$HRI = \frac{EDI}{RFD} \qquad \text{(EQ 3)}$$

In this study, RfD (reference dose) for NO_3^- and F^- were 1.6 and 0.06 mg/kg/day, respectively. An HRI value of <1 indicates no risk, whereas an HRI value of >1 suggests that the likelihood of non-carcinogenic risk exceeds the acceptable level. The overall hazard index is the cumulative HQ for both NO_3^- and F^-.

2.4 Statistical and Spatial Analysis

Bivariate plots were made using Microsoft Excel Software (Microsoft 365 ProPlus), correlation matrices were determined using SPSS statistics V20, and ternary plots were generated using Diagrammes software. To assess the spatial distribution of the various contaminants, concentration maps were made using Arc GIS 10.1. In addition, geochemical modeling and saturation indices of minerals and fluoride species were also calculated using PHREEQC Interactive 2.11.

3 Results and Discussions

3.1 Groundwater Chemistry, spatial distribution, and enrichment of NO_3^-, SO_4^{2-}, Cl^- and F^-

Summaries of groundwater pH, depth, EC, TDS, and minimum, maximum, mean, and standard deviation (SD) values for the ionic concentrations are given in Table 1. The ESR groundwater is neutral to alkaline, with a pH range of 7.0 to 8.8 and the CSR groundwater is acidic to moderately alkaline (pH range 5.7 to 7.5). The pH of TSR is highly alkaline (7.8-8.8) with two wells exceeding the WHO limit of 6.5-8.5. The acidic pH of CSR may be due to coal seams that generate acidity. Well depths were 6-137 m, 21-137 m, and 131-144 m for the ESR, CSR and TSR, respectively. Electrical conductivity values ranged between 619-2910 µS/cm, 330-1290 µS/cm, and 1142-1740 µS/cm for the three areas, respectively. Approximately 57% and 2% of the tested ESR and CSR wells, respectively were above the permissible limit of 1000 µS/cm. However, all the tested wells of TSR were above the WHO drinking water quality standard of 1000 µS/cm (Table 1). Relatively shallow water and semi-arid climatic conditions of ESR and CSR depicts low mineralization and less EC as compare to TSR where prevailing arid and hot environment resulted in higher concentrations of salts in the deeper groundwater. Total dissolved solids (TDS) of the ESR and TSR samples were in the range of 312-2050 mg/L and 894-1290 mg/L, respectively, with 24% ESR samples and 91% TSR samples above the WHO recommended value of 1000 mg/L (WHO 2011). By comparison, The TDS of the CSR samples, with a range of 234-920 mg/L, were within the permissible limit.

Na^+, with mean concentrations of 25 mg/L, 93 mg/L and 166 mg/L in the ESR, CSR and TSR samples, is the most dominant cation, followed by Ca^{2+} and Mg^{2+} (Table 1). Concentrations of Ca^{2+} were 18-158 mg/L, 31-183 mg/L and 46-71 mg/L for the ESR, CSR and TSR samples, respectively. Likewise, Mg^{2+} concentration ranges were 8-99 mg/L, 17-59 mg/L, and 56-148 mg/L in the ESR, CSR and TSR samples, respectively. Elevated concentrations of K^+, with observed ranges of 0.3-55 mg/L and 2-42 mg/L, were found in the ESR and CSR samples. By contrast, the

TSR samples had K^+ concentrations that were within the permissible limit of 12 mg/L (WHO 2011). Ghazi and Mountney (2011) proposed that elevated cation concentrations were mainly due to cation exchange and dissolution of parent minerals embedded with the coal seams (Ghazi and Mountney 2011).

Spatial distributions of NO_3^-, SO_4^{2-}, Cl^- and F^- are shown in Fig. (1). Groundwater NO_3^- concentrations varied widely, from 0.2-308 (mean 58.5) mg/L in the ESR samples, to 2.7-203 (73.4) mg/L in the CSR samples to 1.1-259 (mean 68.4) mg/L in the TSR samples. Approximately 16% of the ESR, 32% of the CSR, and 18% of the TSR samples have NO_3^- concentrations higher than 100 mg/L, i.e. twice the WHO-recommended value of 50 mg/L.

Groundwater F^- concentrations ranged from 0.1-1.8 mg/L (mean 0.6 mg/L), 0.1-2.7 mg/L (mean 0.9 mg/L) and 0.3-2.5 mg/L (mean 1.6 mg/L) in the ESR, CSR and TSR samples, respectively (Fig. 1). Likewise, higher groundwater SO_4^{2-} and Cl^- were also observed in the coal mining areas of Salt Range, Pakistan. Sulfate concentrations varied from 14-190 mg/L (mean value 99 mg/L) for the ESR samples, 30-580 mg/L (mean 144 mg/L) for the CSR samples, and 160-618 mg/L (mean of 314 mg/L) for the TSR samples. The groundwater ESR, CSR and TSR Cl^- concentrations ranged from 0-423 mg/L (mean 110 mg/L), 6.2-423 mg/L (mean 77.2 mg/L) and 38-230 mg/L (mean 102 mg/L), respectively. Elevated concentrations of Cl^- are probably due to the geological settings of Salt Range i.e. the presence of huge rock salt and gypsum deposits in the area (Batool et al. 2018).

Many ESR, CSR and TSR samples had NO_3^- concentrations that were several fold higher than the WHO recommended value of 50 mg/L. Sulfate concentrations were also two times higher than the WHO guideline of 250 mg/L in the CSR and TSR samples, and Cl^- concentrations were two times

the guideline value of 250 mg/L in the ESR and TSR samples. Three %, 17 %, and 27 % of the ESR, CSR, and TSR samples, respectively, also exceeded the WHO prescribed F^- limit of 1.5 mg/L. Since Cl^- and NO_3^- are relatively smaller in size and are more mobile than larger sulfate ions and other mining contaminants, the high Cl^- and NO_3^- concentrations may be linked to human health concerns (Bosman 2009).

3.2 Nitrate geochemistry and sources: role of mining practices

Forty-one percent, 57 % and 36% of samples of the ESR, CSR and TSR exceeded the WHO and Pak-NEQs permissible limit of 50 mg/L NO_3^- (Parvaiz et al. 2020; WHO 2011). The extent to which NO_3^- is enriched in water is mainly dependent on source contributions, environmental factors (temperature and precipitation) and physio-chemical parameters such as pH, depth, EC, TDS and anion proxies such as Cl^- and SO_4^{2-} (Rawat *et al*. 2019).
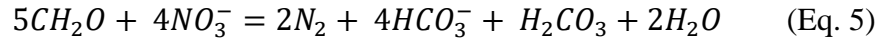
The main sources of groundwater nitrate contamination include natural sources such as atmospheric deposition and nitrification of organic nitrogen in soils, and anthropogenic sources including manure, industrial and municipal sewage, agricultural runoff, burning of fossil fuels as well as coal mining activities (Nyilitya et al. 2020). Positive associations between TDS and high NO_3^- or SO_4^{2-} suggests dominance of anthropogenic sources (Ramaroson et al. 2020). In this study TDS showed a positive correlation with SO_4^{2-} (ESR $r^2 = 0.4$) and a significant positive correlation for CSR and TSR ($r^2 = 0.5$), whereas TDS showed a weak positive correlation with NO_3^- ($r^2=0.3$ for ESR, and $r^2=0.4$ for CSR). These weak positive correlations (Table 2 (a, b & c) suggest that the groundwater was mainly influenced by anthropogenic activities. Such anthropogenically-derived NO_3^- surface and/or atmospheric deposition has been shown to mostly contaminate shallow wells (mean depth <60 m) (Long and Luo 2020). However, in our study, NO_3^-

concentrations were high both in shallow (mean depth <60 m) and deeper wells with mean depths of >60 m (Fig. 3). Such contamination patterns could be indicative of anthropogenically induced leaching of geological sources such as coal (Long and Luo 2020).

Bivariate NO_3^-/Cl^- vs Cl^- plots can also be used for source apportionment as well as to define the control of different biological processes (e.g. nitrification, denitrification, assimilation, and mineralization) responsible for nitrate geochemistry (Ogrinc et al. 2019). High NO_3^-/Cl^- and high Cl^- suggest agricultural input, low NO_3^-/Cl^- and high Cl^- point to municipal/domestic sources and high NO_3^-/Cl^- and relatively low Cl^- suggest geochemical sources (Ogrinc et al. 2019). In our study, the NO_3^-/Cl^- versus Cl^- plot showed that most of the samples were in the high NO_3^-/Cl^- and low Cl^- category (Fig. 2). As coal mining is the primary activity disturbing the geological setting in the study area, this geochemically bounded nitrate could have been leached into groundwater during coal excavation. Additionally, 12% of the ESR samples and 7% of CSR samples showed increasing Cl^- with decreasing NO_3^-/Cl^- (Fig. 2), which suggests that denitrification and dilution processes may have minimized NO_3^- loading profiles in the study area (Nyilitya et al. 2020). Thus, high NO_3^- in both shallow and deep groundwaters suggested that coal exploration may have recharged the adjacent aquifers with elevated NO_3^-.

Interrelationships between NO_3^- and Cl^- can also be used as an indicator to differentiate various sources of nitrate contamination. High NO_3^- and Cl^- concentrations reflect anthropogenic sources that could be coal mining activities whereas low Cl^- and high NO_3^- concentrations suggest agricultural inputs (Kanagaraj and Elango 2016). The CSR samples showed positive correlations between NO_3^- and Cl^- ($r^2=0.4$) and the TSR samples showed significant positive correlations ($r^2=0.6$). These positive correlations imply that anthropogenic sources in the study (which could be the coal mining activities) could have induced dissolution of Cl^- and NO_3^- containing minerals

12

to release NO_3^- (Kanagaraj and Elango 2016). However, relatively low values of NO_3^- and high values Cl^- in the ESR samples may reflect dilution as a controlling factor for nitrate loadings. The dilution occurs primarily as denitrification and is limited by pH (Eq 4 & 5).

$$NO_3^- + H^+ + H_2O = NH_3 + 2O_2 \qquad \text{(Eq. 4)}$$

$$5CH_2O + 4NO_3^- = 2N_2 + 4HCO_3^- + H_2CO_3 + 2H_2O \qquad \text{(Eq. 5)}$$

Denitrification of nitrate occurs in alkaline pH solutions, (Eq. 4), whereas nitrate mobilization via nitrification processes occurs in acidic and reduced environments (Eq. (5); Bosman 2009). This inverse relationship between NO_3^- and pH for the ESR samples suggests that denitrification was likely occurring in the study area (Fig. 3). In the case of CSR and TSR sites, however, a very weak positive correlation between pH and NO_3^- and a positive correlation of NO_3^- and HCO_3^- (r^2=0.5 for CSR and 0.4 for TSR) suggest that denitrification was not occurring in these areas. Therefore, elevated concentrations in these areas could have been the product of nitrification (Rezaei et al. 2017).

The N cycle can also be affected by acidification. High sulfate concentrations are a primary indicator of acid mine drainage. Sulfate, upon reaction with water, produces H_2SO_4 and enhances acidification. Similar to the SO_4^{2-}, the bedrock nitrogen bearing minerals, upon coal excavation via oxidation, process produce nitrates which dissolve in the surrounding waters at a rate higher than the sulfates (Bosman 2009). The positive association between SO_4^{2-} and NO_3^- provides additional evidence that exploitation of coal and weathering of mined waste oxidized the fixed nitrogen content of the coal and other parental minerals that acted as sources of NO_3^- contamination in the area (Fig. 2). Therefore, the overall high contents of SO_4^{2-}, NO_3^- and Cl^- could be an indication of coal mining associated water concerns, as oxidation of pyrite and dissolution of

sulfate bearing secondary minerals in the coals could have been hosts of nitric and hydrofluoric acid as well as elevated groundwater SO_4^{2-}. The prolonged mining practices are the only process by which the geological bedrock is disturbed in the study area, and this likely intensified the oxidizing conditions that were the possible reason behind the nitrification.

3.3 Geochemistry and source of groundwater fluoride

The main source of groundwater F^- contamination is the dissolution of fluorine-containing minerals such as fluorite (CaF_2), gypsum and clay minerals (Rezaei et al. 2017). This is mainly controlled by the parent minerals, the residence time of water-rock interaction, pH, and temperature as well as ion exchange capacity of the water environment (Younas et al. 2019). pH is one of the major controls that governs the dissolution and mobility of F^-, and high pH conditions, in particular, can facilitate adsorption and desorption. For instance, at alkaline pH values, the cation exchange and dissolution of F^- bearing minerals by replacing the hydroxyl ion with F^- ion facilitates the F^- release (Eq. 6) (Younas et al. 2019).

$$KAl_2[AlSi_3O_{10}]F_2 + 2OH^- = KAl_2[AlSi_3O_{10}][OH]_2 + 2F^- \qquad (Eq.\,6)$$
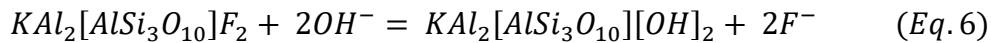
By contrast, low pH conditions favour the dissolution of calcium rich minerals such as calcite, resulting in the release of Ca^{2+} that can precipitate with F^- to form CaF_2 and thus lower groundwater F- concentraitons (Eq. 7) (Yadav et al. 2020).

$$CaCO_3 + 2F^- + H^+ = CaF_2 + 2HCO_3^- \qquad (Eq.\,7)$$

In this study alkaline pH and high fluoride concentrations were reported in waters from the ESR and TSR sites. There was a weak positive correlation between pH and F^- in the ESR samples ($r^2=0.3$), and a significant positive correlation for these parameters in the TSR samples ($r^2=0.8$).

14

The CSR samples had acidic pH and elevated groundwater F^- concentrations. This unusual behavior is proposed to be mainly associated with coal mining activities in this area. Oxidation of pyrite in the coal would have produced H_2SO_4,. Analysis of XRD data for coal samples from the study area (Online *Source* 2) showed that kaolinite, illite, chlorite, and muscovite minerals were present. These may have been the main hosts of fluoride (Luo et al., 2018). Dissolution of these coal minerals by the sulfuric acid could have released the F^- (Xiong et al. 2017). Subsequently, the F^- may have reacted with the sulfuric acid to produce HF (Eq 8, 9). This hypothesis is supported by significant positive correlations between F^- and SO_4^{2-} (r^2=0.7) for the CSR waters (Fig. 4). Thus, oxidation of sulfide minerals was probably the common source for acidity and elevated F^- levels in the study area (Fig. 4).

Competitive adsorption of F^- with other anions such as HCO_3^- could also affect the groundwater chemistry. Bicarbonate ion is able to compete with F^- for the active sites in minerals, which in turn could result in enhance groundwater F^- (Eq. 8).

$$CaF_2 + HCO_3^- = CaCO_3 + H^+ + 2F^- \qquad \text{(Eq. 8)}$$
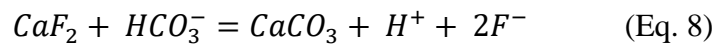
The slightly positive correlation of F^- with HCO_3^- in ESR site (r^2= 0.3) suggests such competitive exchange. By comparison, relatively high values of HCO_3^- with low F^- concentrations in the CSR and TSR samples contradict this competitive adsorption mechanism in these areas (Fig. 4).

The ion exchange ability of Na^+ and Ca^{2+} in the weathering zone of groundwater aquifers may also enhance F^- dissolution (Younas et al. 2019). The dissolution of CaF_2 can results in enrichments of F- in groundwater (Eq. 8). Similarly, positive associations between Na^+ and F^- suggest that elevated levels of Na^+ also favors groundwater F^- mobility in alkaline pH solutions (Luo et al., 2018). In our study F^- showed a negative correlation with Ca^{2+} (r^2=-0.3 for ESR and CSR and r^2=

-0.6 for TSR) and a slight positive association with Na^+ (r^2=0.3 for ESR) (Table 2). The elevated concentrations of Na^+ and lower Ca^{2+} concentrations in the CSR and TSR samples implies that cation exchange mechanism may have caused the high groundwater F^- in the study area (Table 1). However, the inverse trend observed in the ESR site suggested that the dissolution of calcium may have enhanced F^- release over time (Fig. 5).

It has been postulated that a positive correlation of F^- with TDS and SO_4^{2-} indicates that salt formation could be another controlling factor for groundwater F^- contamination (Yadav et al. 2020). The major salt responsible for such reactions are halite and gypsum (Luo et al. 2018), and the precipitation and evaporation of these minerals can mobilize groundwater F^-. The weak positive correlation between F^- and depth (r^2=0.3 for ESR and CSR) and significant positive correlation in the TSR samples (r^2=0.5) also suggests that dissolution of calcium/magnesium rich bedrock geochemistry could have had direct influence on F^- contamination in the deeper wells (Fig. 4).

To explore possible mechanisms of F- contamination further, saturation indices (SIs) of the groundwater samples were calculated, and the results are shown in the supplementary data (Online *Source* 1). Samples with SI values < 0 suggest undersaturation with respect to calcite, dolomite, fluorite, gypsum, and halite. This in turn implies that these minerals may have dissolved and released Ca^{2+}, Mg^{2+}, Na^+ and SO_4^{2-} that may have mobilized groundwater F- during cation exchange (Eq 6,7, 8).

Anthropogenic activities such as fertilizer applications, sewage release, industrial waste discharge and coal mining/burning may cause fluoride contamination (Luo et al. 2018). In our study (*Section* 3.2) agricultural and sewage inputs were unlikely sources of F^-. The weak but positive relationship

16

between F^- and NO_3^- (r^2=0.3) suggested a common source of contamination that was probably anthropogenic. As coal mining is the primary activity in the study area it could be considered as this anthropogenic source.

3.4 Pollution Index and Human Health Risk Assessment

Calculated Pollution Indices (PI) for NO_3^-, F, EC, Cl$^-$, and SO_4^{2-} were all greater than 1 (Fig. 5a), suggesting samples are significantly polluted. The elevated concentrations of NO_3^- and F^- ions may pose serious human health risks. The health risk index (HRI) of these two groundwater priority pollutants via drinking water was assessed for different age groups including adults, children, and minors (Fig. 5b). The groundwater F^- and NO_3^- health risks of coal mining areas of Salt Range were classified into three classes HRI<1= safe drinking water, HRI>1 as high, and HRI>5 as alarmingly high risk. The HRI for F^- >1 at all sites followed the sequence of CSR>TSR>ESR. The hazard index of F demonstrated that CSR and TSR sites having ranges between 0-2.1, 0-2.6 0-9.5, and 0-2, 0-2.4, and 0-8.8 for adults, children, and infants were most susceptible. This is similar to the risk for NO_3^-. Mean HRIs of 8 (range 0.5-21.6) mg/kg/d for adults, 8.7 (range 0.6-26) mg/kg/d children, and 36 (range 2.3-97.3) mg/kg for infants were calculated for the TSR samples. These HRIs were higher than those for the ESR samples (mean 1.7 (range 0-9.1), mean 2 (0-10.9) and mean 7.5 (range 0-41) mg/kg/d for adults, children, and infants, respectively). On comparison the hazard index in ESR site had lower ranges for F (0-1.4, 0-1.7 and 0-6.4) while CSR had low values for NO_3^- having range of 0.6-6.1 (mean 2.2), 0.1-7.2 (mean 2.2) and 0.4-27 (mean 9.7) mg/kg/d for adults, children, and infants, respectively. These results suggest that among the different groups of ages, infants with the weak immune system and lower body weights are at higher risk than the children and adults. The potential health risk of these excessively elevated levels of F^- and NO_3^- include dental and skeletal fluorosis, methemoglobinemia in infants and cancer, and mucous

17

membrane irritation in adults (Younas et al. 2019; Ako et al. 2014). Overall, the study suggests that a non-acceptable carcinogenic risk associated with drinking water NO_3^- and F^- in the Salt Range, Punjab may exist.

Conclusions

In the Salt Range, Punjab, Pakistan, groundwater NO_3^- and F^- were derived from natural and anthropogenic sources. Groundwater NO_3^- contamination is mainly associated with geogenic sources especially coals and bedrock geology. Higher values of SO_4^{2-}, NO_3^- and Cl^- imply that anthropogenic sources in the study could have induced dissolution of Cl^- and NO_3^- containing minerals to release NO_3^-. In addition, oxidizing conditions were the possible reason behind nitrification. Similarly, muscovite, illite and calcite were the most dominant mineralogical signatures found in the lithological units of the present study area were the main source of fluoride enrichment. Saturation index of calcite, dolomite, fluorite, gypsum and halite (SI\0) also revealed that dissolution and mineralization of Ca^{2+}, Mg^{2+}, Na^+ and SO_4^{2-} most likely mobilized groundwater F- during cation exchange. Oxidation of sulfide minerals was probably the common source for acidity and another possible source of elevated F^- and NO_3^- levels. Such circumstances revealed that as coal mining is the primary activity disturbing the geological setting in the study area, the geochemically bounded NO_3^- and F^- could have been leached into groundwater during coal excavation. The potential health risk of elevated concentrations of NO_3- and F^- in different age groups were above calculated limits and the results indicate that infants may be most at risk. Therefore, precautionary measurements should be taken by the local authorities to set an alert for NO_3^- and F^- and infants and pregnant women should be provided with an alternative source of drinking water.

Acknowledgements

Conflict of interest/Competing Interest

The authors declare that there is no conflict of interest.

Availability of data and material

Supplementary data are provided along with the manuscript.

Code Availability

Not applicable.

Author Contributions

Noshin Masood (Environmental Geochemistry Laboratory, Department of Environmental Sciences, Faculty of Biological Sciences, Quaid-i-Azam University) conducted the research, interpreted the data, and wrote the manuscript.

Prof. Karen Hudson-Edwards (Professor in Sustainable Mining, Environment and Sustainability Institute and Camborne School of Mines and, University of Exeter) assisted with analytical work and the writing of the manuscript.

Dr. Abida Farooqi (Associate Professor in Environmental Geochemistry Laboratory, Department of Environmental Sciences, Faculty of Biological Sciences, Quaid-i-Azam University) is the corresponding author and provided technical assistance in developing the manuscript.

References

Ako, A. A., Eyong, G. E. T., Shimada, J., Koike, K., Hosono, T., Ichiyanagi, K., et al. (2014). Nitrate contamination of groundwater in two areas of the Cameroon Volcanic Line (Banana Plain and Mount Cameroon area). *Applied Water Science, 4*(2), 99-113.

APHA (2005). Standard methods for the examination of water wastewater. *21*, 258-259.

Bailey, B., Smith, L., Blowes, D., Ptacek, C., Smith, L., & Sego, D. (2013). The Diavik Waste Rock Project: Persistence of contaminants from blasting agents in waste rock effluent. *Applied Geochemistry, 36*, 256-270.

Batool, A., Aziz, S., & Imad, S. (2018). Physico-chemical quality of drinking water and human health: a study of salt range Pakistan. *International Journal of Hydrology, 2*(6), 668-677.

Bodrud-Doza, M., Islam, A. T., Ahmed, F., Das, S., Saha, N., & Rahman, M. S. (2016). Characterization of groundwater quality using water evaluation indices, multivariate statistics and geostatistics in central Bangladesh. *Water Science, 30*(1), 19-40.

Bosman, C. (2009). The Hidden Dragon: Nitrate Pollution from Open-pit Mines–A case study from the Limpopo Province, South Africa. *Carin Bosman Sustainable Solutions Pretoria, Gauteng, Republic of South Africa.* (Vol. 26442).

Chen, J., Wu, H., Qian, H., & Gao, Y. (2017). Assessing nitrate and fluoride contaminants in drinking water and their health risk of rural residents living in a semiarid region of Northwest China. *Exposure Health, 9*(3), 183-195.

Daud, M., Nafees, M., Ali, S., Rizwan, M., Bajwa, R. A., Shakoor, M. B., et al. (2017). Drinking water quality status and contamination in Pakistan. *BioMedical Research International, 2017*.

Derakhshani, R., Raoof, A., Mahvi, A. H., & Chatrouz, H. (2020). Similarities in the fingerprints of Coal mning activities, high ground water fluoride, and dental fluorosis in Zarand District, Kerman Province, Iran. *Fluoride, 53*(2 Pt 1), 257-267.

Endale, D. M., Potter, T. L., Strickland, T. C., & Bosch, D. D. (2017). Sediment-bound total organic carbon and total organic nitrogen losses from conventional and strip tillage cropping systems. *Soil Tillage Research, 171*, 25-34.

Essilfie-Dughan, J., Hendry, M. J., Dynes, J. J., Hu, Y., Biswas, A., Barbour, S. L., et al. (2017). Geochemical and mineralogical characterization of sulfur and iron in coal waste rock, Elk Valley, British Columbia, Canada. *Science of The Total Environment, 586*, 753-769.

Ghazi, S., & Mountney, N. P. (2011). Petrography and provenance of the Early Permian Fluvial Warchha Sandstone, Salt Range, Pakistan. *Sedimentary Geology, 233*(1-4), 88-110.

Guohua, L., Qiyan, F., Xiaoli, D., Yahong, C., Wenbo, L., Hui, W., et al. (2019). Geochemical characteristics of fluorine in coal within Xiangning mining area, China, and associated mitigation countermeasures. *Energy Exploration, 37*(6), 1737-1751.

Hendry, M. J., Wassenaar, L. I., Barbour, S. L., Schabert, M. S., Birkham, T. K., Fedec, T., et al. (2018). Assessing the fate of explosives derived nitrate in mine waste rock dumps using the stable isotopes of oxygen and nitrogen. *Science of The Total Environment, 640*, 127-137.

Jahangir, M. M., Johnston, P., Khalil, M. I., & Richards, K. G. (2012). Linking hydrogeochemistry to nitrate abundance in groundwater in agricultural settings in Ireland. *Journal of Hydrology, 448*, 212-222.

Kanagaraj, G., & Elango, L. (2016). Hydrogeochemical processes and impact of tanning industries on groundwater quality in Ambur, Vellore district, Tamil Nadu, India. *Environmental Science Pollution Research, 23*(23), 24364-24383.

Katz, B. G., Chelette, A. R., & Pratt, T. R. (2004). Use of chemical and isotopic tracers to assess nitrate contamination and ground-water age, Woodville Karst Plain, USA. *Journal of Hydrology, 289*(1-4), 36-61.

Kuter, N., Dilaver, Z., & Gül, E. J. I. J. o. M., Reclamation (2014). Determination of suitable plant species for reclamation at an abandoned coal mine area. *International Journal of Mining, Reclamation Environmental Earth Sciences, 28*(5), 268-276.

Li, X., Wu, P., Han, Z., & Shi, J. (2016). Sources, distributions of fluoride in waters and its influencing factors from an endemic fluorosis region in central Guizhou, China. *Environmental Earth Sciences, 75*(11), 981.

Long, J., & Luo, K. (2020). Elements in surface and well water from the central North China Plain: Enrichment patterns, origins, and health risk assessment. *Environmental Pollution, 258*, 113725.

Luo, W., Gao, X., & Zhang, X. (2018). Geochemical processes controlling the groundwater chemistry and fluoride contamination in the Yuncheng Basin, China—An area with complex hydrogeochemical conditions. *PloS One, 13*(7), e0199082.

Mahmood, F. N., Barbour, S. L., Kennedy, C., & Hendry, M. J. (2017). Nitrate release from waste rock dumps in the Elk Valley, British Columbia, Canada. *Science of the Total Environment, 605*, 915-928.

Malek Mohammadi, T., Derakhshani, R., Tavallaie, M., Raoof, M., Hasheminejad, N., & Haghdoost, A. A. (2017). Analysis of ground water fluoride content and its association with prevalence of fluorosis in Zarand/Kerman:(using GIS). *Journal of Dental Biomaterials, 4*(2), 379.

Masilionytė, L., Maikštėnienė, S., Velykis, A., & Satkus, A. (2014). Agroecosystems to decrease diffuse nitrogen pollution in northern Lithuania. *Journal of Environmental Engineering Landscape Management, 22*(3), 194-207.

Nephalama, A., & Muzerengi, C. (2016). Assessment of the influence of coal mining on groundwater quality: Case of Masisi Village in the Limpopo Province of South Africa. *Proceedings of the Freiberg/Germany, Mining Meets Water—Conflicts Solutions , Leipzig, Germany* (pp. 11-15).

Nyilitya, B., Mureithi, S., & Boeckx, P. (2020). Tracking Sources and Fate of Groundwater Nitrate in Kisumu City and Kano Plains, Kenya. *Water, Air Soil Pollution: Focus, 12*(2), 401.

Ogrinc, N., Tamše, S., Zavadlav, S., Vrzel, J., & Jin, L. (2019). Evaluation of geochemical processes and nitrate pollution sources at the Ljubljansko polje aquifer (Slovenia): A stable isotope perspective. *Science of The Total Environment, 646*, 1588-1600.

Parvaiz, A., Khattak, J. A., Hussain, I., Masood, N., Javed, T., & Farooqi, A. (2020). Salinity enrichment, sources and its contribution to elevated groundwater arsenic and fluoride levels in Rachna Doab, Punjab Pakistan: Stable isotope (δ2H and δ18O) approach as an evidence. *Environmental Pollution*, 115710.

Ramaroson, V., Randriantsivery, J. R., Rajaobelison, J., Fareze, L. P., Rakotomalala, C. U., Razafitsalama, F. A., et al. (2020). Nitrate contamination of groundwater in Ambohidrapeto–Antananarivo-Madagascar using hydrochemistry and multivariate analysis. *Applied Water Science, 10*(7), 1-13.

Ravindra, K., & Mor, S. (2019). Distribution and health risk assessment of arsenic and selected heavy metals in Groundwater of Chandigarh, India. *Environmental Pollution, 250*, 820-830.

Rawat, K. S., Jeyakumar, L., Singh, S. K., & Tripathi, V. K. (2019). Appraisal of groundwater with special reference to nitrate using statistical index approach. *Groundwater for Sustainable Development, 8*, 49-58.

Rezaei, M., Nikbakht, M., & Shakeri, A. (2017). Geochemistry and sources of fluoride and nitrate contamination of groundwater in Lar area, south Iran. *Environmental Science and Pollution Research, 24*(18), 15471-15487.

Rivett, M., Smith, J., Buss, S., & Morgan, P. (2007). Nitrate occurrence and attenuation in the major aquifers of England and Wales. *Quarterly Journal of Engineering Geology Hydrogeology, 40*(4), 335-352.

Roy, S., Speed, C., Bennie, J., Swift, R., & Wallace, P. (2007). Identifying the significant factors that influence temporal and spatial trends in nitrate concentrations in the Dorset and Hampshire Basin Chalk aquifer of Southern England. *Quarterly Journal of Engineering Geology Hydrogeology, 40*(4), 377-392.

Sadasivam, S., Thomas, H. R., Zagorščak, R., Davies, T., & Price, N. (2019). Baseline geochemical study of the Aberpergwm mining site in the South Wales Coalfield. *Journal of Geochemical Exploration, 202*, 100-112.

Shukla, S., & Saxena, A. (2018). Global status of nitrate contamination in groundwater: its occurrence, health impacts, and mitigation measures. *Handbook of Environmental Materials Management*, 869-888.

Stone, A., & Edmunds, W. (2014). Naturally-high nitrate in unsaturated zone sand dunes above the Stampriet Basin, Namibia. *Journal of Arid Environments, 105*, 41-51.

Stuart, M., Gooddy, D., Bloomfield, J., & Williams, A. (2011). A review of the impact of climate change on future nitrate concentrations in groundwater of the UK. *Science of The Total Environment, 409*(15), 2859-2873.

Tew, K. (2018). Fetter CW, Boving T, Kreamer D (eds): Contaminant Hydrogeology. *Environmental Earth Sciences, 77*(22), 745.

Villeneuve, S., Barbour, S., Hendry, M., & Carey, S. (2017). Estimates of water and solute release from a coal waste rock dump in the Elk Valley, British Columbia, Canada. *Science of The Total Environment, 601*, 543-555.

Ward, M. H., DeKok, T. M., Levallois, P., Brender, J., Gulis, G., Nolan, B. T., et al. (2005). Workgroup report: drinking-water nitrate and health—recent findings and research needs. *Environmental Health Perspectives, 113*(11), 1607-1614.

Warwick, P. D., Shakoor, T., Javed, S., Mashhadi, S., Hussain, H., Anwar, M., et al. (1990). Chemical and physical characteristics of coal and carbonaceous shale samples from the Salt Range coal field, Punjab Province, Pakistan. US Geological Survey.

WHO, G. J. W. H. O. (2011). Guidelines for drinking-water quality. (Vol. 216, pp. 303-304).

Wu, D., Zheng, B., Tang, X., Li, S., Wang, B., & Wang, M. (2004). Fluorine in Chinese coals. *Fluoride, 37*, 125-132.

Xiong, Y., Xiao, T., Liu, Y., Zhu, J., Ning, Z., & Xiao, Q. (2017). Occurrence and mobility of toxic elements in coals from endemic fluorosis areas in the Three Gorges Region, SW China. *Ecotoxicology Environmental Safety, 144*, 1-10.

Yadav, K., Raphi, M., & Jagadevan, S. (2020). Geochemical appraisal of fluoride contaminated groundwater in the vicinity of a coal mining region: Spatial variability and health risk assessment. *Geochemistry*, 125684.

Yang, Y., Guo, T., & Jiao, W. (2018). Destruction processes of mining on water environment in the mining area combining isotopic and hydrochemical tracer. *Environmental Pollution, 237*, 356-365.

Younas, A., Mushtaq, N., Khattak, J. A., Javed, T., Rehman, H. U., & Farooqi, A. (2019). High levels of fluoride contamination in groundwater of the semi-arid alluvial aquifers, Pakistan: evaluating the recharge sources and geochemical identification via stable isotopes and other major elemental data. *Environmental Science Pollution Research, 26*(35), 35728-35741.

Zaitsev, G., Mettänen, T., & Langwaldt, J. (2008). Removal of ammonium and nitrate from cold inorganic mine water by fixed-bed biofilm reactors. *Minerals Engineering, 21*(1), 10-15.

List of figures

Figure 2: a) Ternary and bivariate plots illustrating NO_3^- sources.

Figure 3: Relationships between concentrations of NO_3^- and Cl^-, EC, pH, HCO_3^-, depth, and SO_4^{2-}.

Figure 4: Relationships between concentrations of F^- and TDS, Cl^-, pH, Na^+, Ca^{2+}, HCO_3^-, SO_4^{2-}, Depth, and NO_3^-.

Figure 5: Pollution Index (PI) of potentially toxic contaminants and b) Health risk Index (HRI) due to groundwater NO_3^-, and F^- contamination.
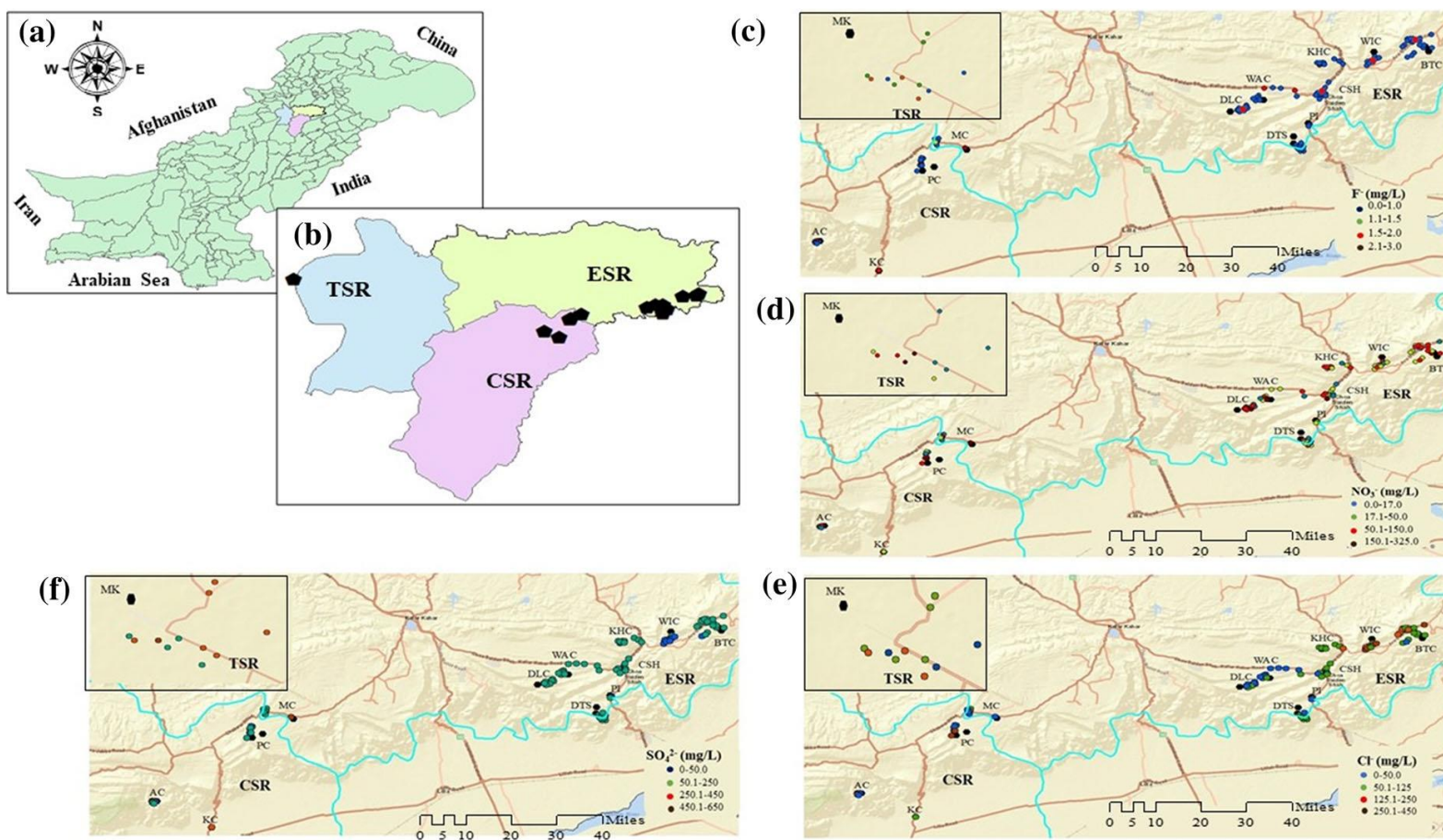
Figure 1: (a and b) sampling locations **(c)** spatial distribution of F^-, **(d)** spatial distribution of NO_3^-, **(e)** spatial distribution of Cl^- and **(f)** spatial distribution of SO_4^{2-}

*ESR= Eastern Salt Range, CSR= Central Salt Range, TSR= Trans-Indus Salt Range. *BTC (Basharat), WIC (Wahali), KHC (Khajula), CSH (Choa Saiden Shah), PIC (Pidh), DTC (Dandot), DLC (Dalwal), and WAC (Wahula) are villages studied under ESR coal mining areas. MC (Munarah), PC (Padhrar), KC (Katta Karli), and AC (Arrara) were studied in CSR. MK (Makarwal) under TSR mining area.
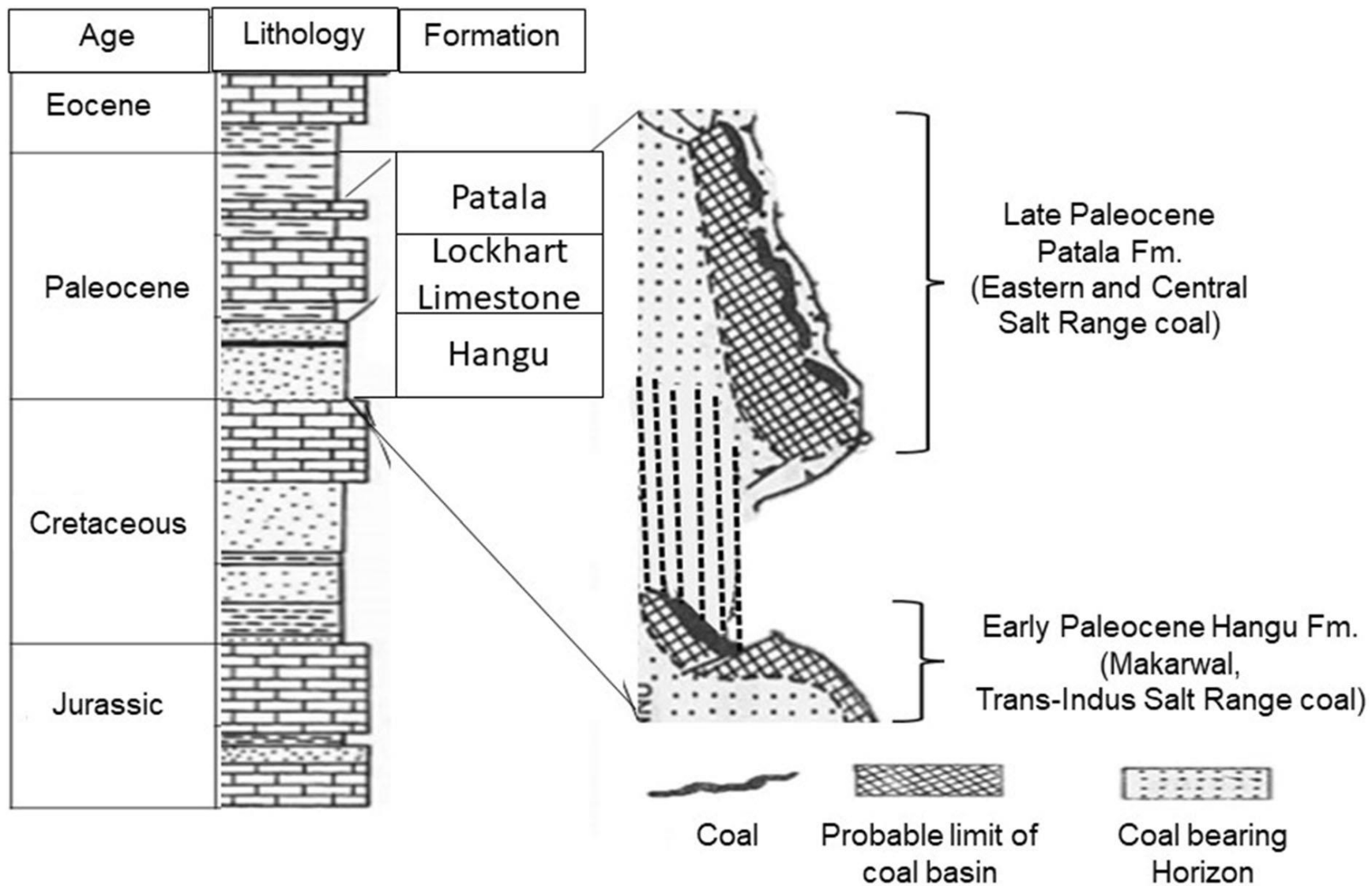
Figure 2. Stratigraphy and lithologies of the Salt Range and the occurrence of coal seams (modified from Malik 1989).

Figure 3. Relationships between concentrations of NO_3^- and Cl^-, EC, pH, HCO_3^-, depth and SO_4^{2-} in the groundwater samples.

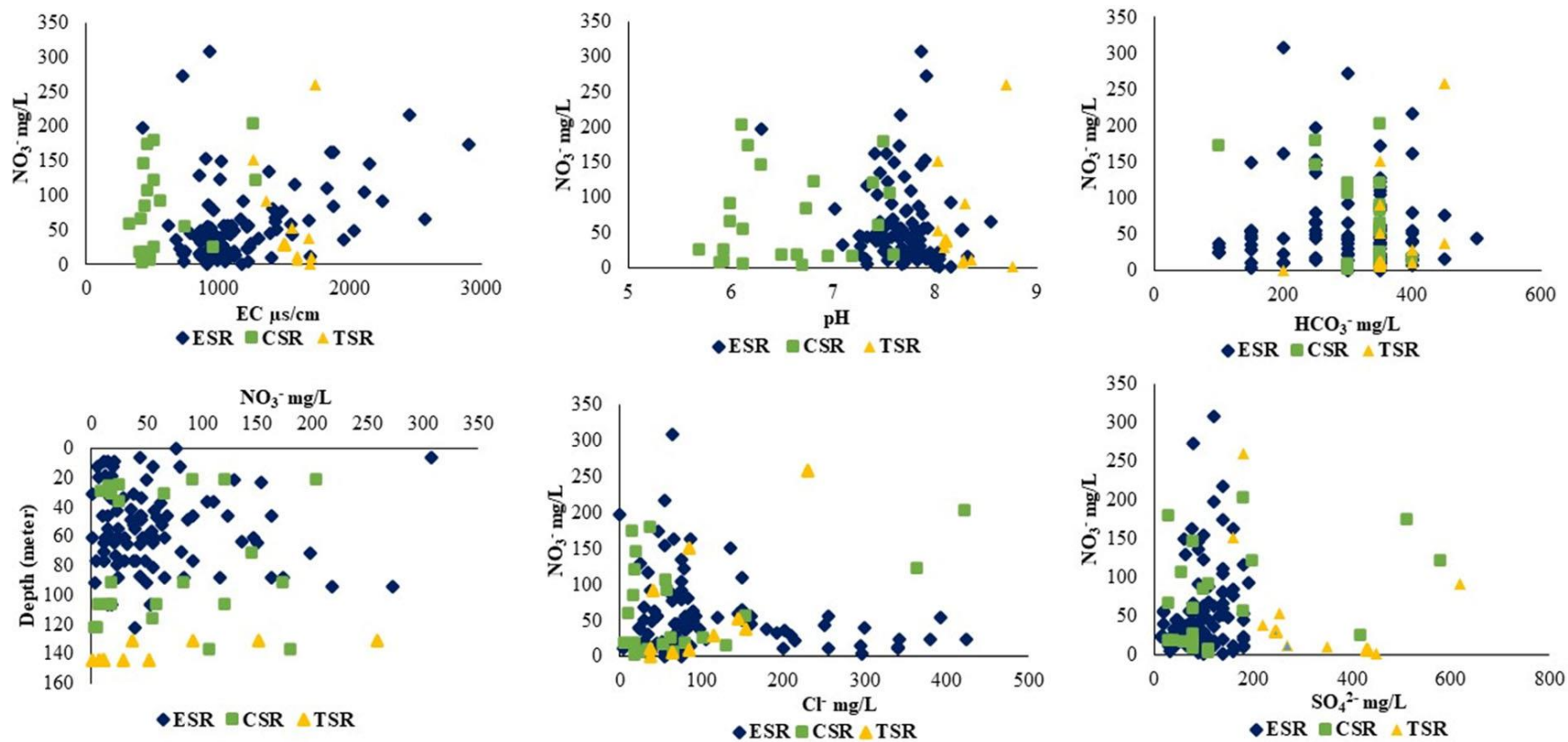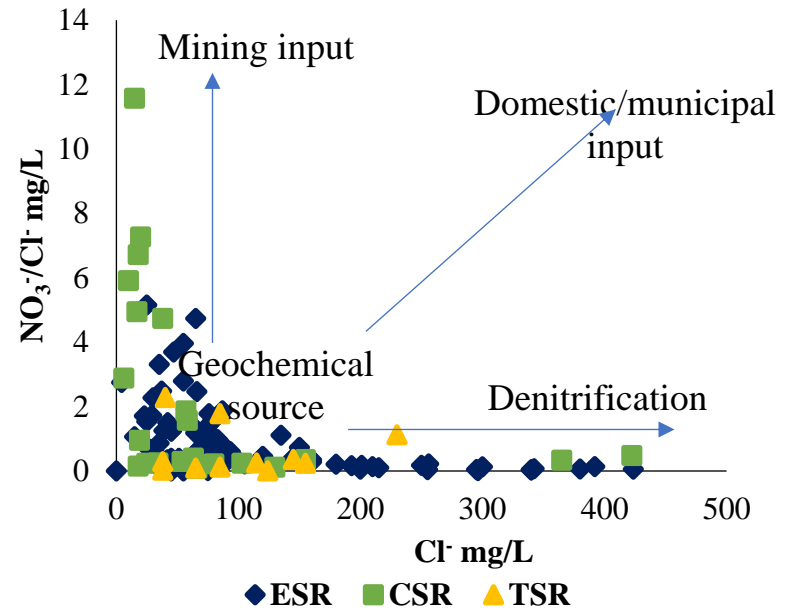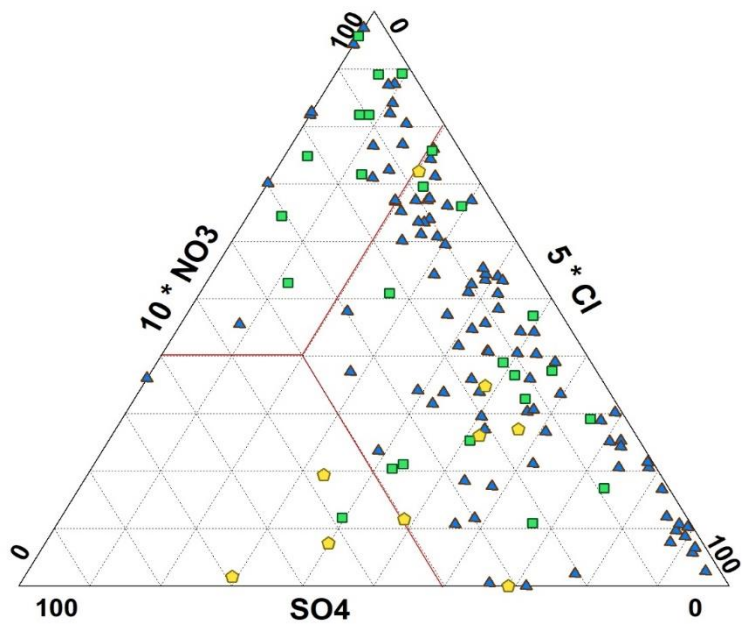**Figure 4: Ternary and bivariate plots illustrating NO₃⁻ sources.**

Figure 3: Relationships between concentrations of NO₃⁻ and Cl⁻, EC, pH, HCO₃⁻, depth, and SO₄²⁻ in the groundwater samples.
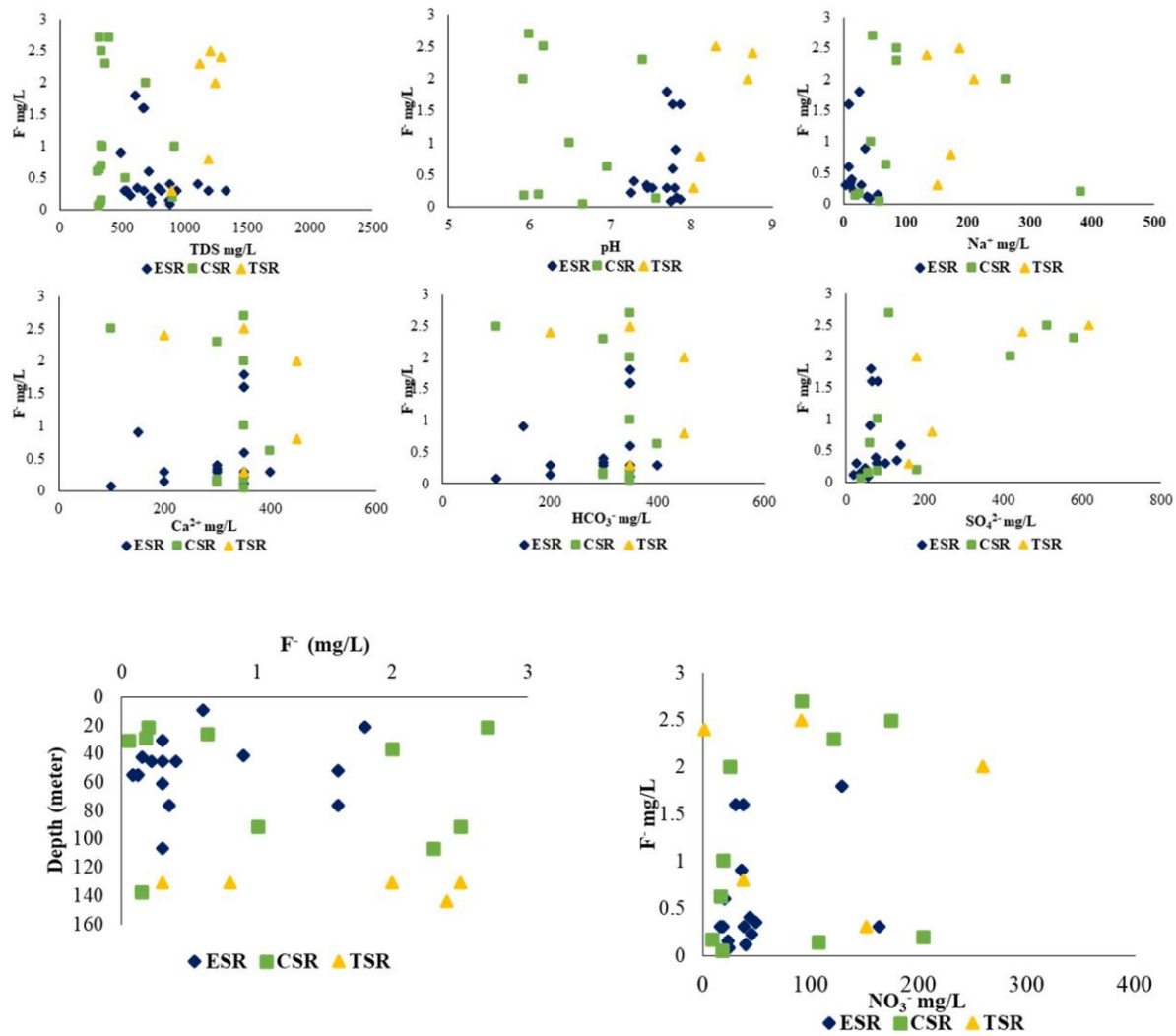
Figure 5: Relationships between concentrations of F⁻ and TDS, Cl⁻, pH, Na⁺, Ca²⁺, HCO₃⁻, SO₄²⁻, depth, and NO₃⁻ in the groundwater samples.
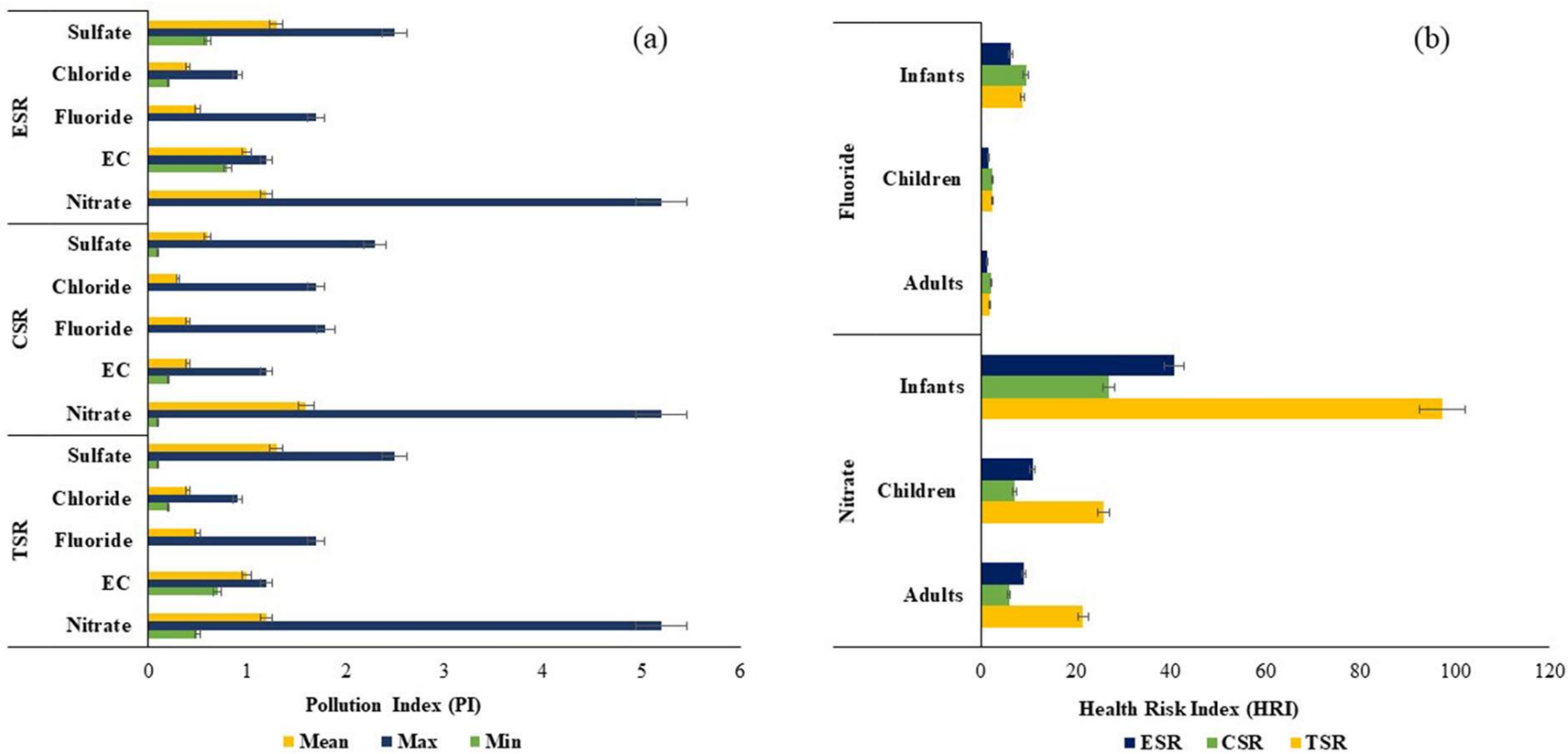
Figure 6. (a) Pollution Index (PI) of potentially toxic contaminants and (b) Health risk Index (HRI) due to groundwater NO_3^- and F^- contamination.

Table 1: Statistical results for physicochemical parameters in coal mining areas of the Salt Range, Punjab.

Sites		Observed Parameters	pH	Depth (m)	TDS (mg/L)	EC (µS/cm)	HCO_3^- (mg/L)	Na^+ (mg/L)	K^+ (mg/L)	Ca^{2+} (mg/L)	Mg^{2+} (mg/L)
WHO limits			6.5-8.5	-	1000	1500	-	200	12	75	50
ESR	(N*= 9) (n*=97)	Min-Max	7.0-8.8	6-122	312-2050	619-2910	100-500	3-84	0.3-55	18-158	8-99
		Mean	7.7	57	839	1204	300	25	8.1	117	49
		SD	0.3	26	308	447	89	18	11	30	20
CSR	(N=4) (n=23)	Min-Max	5.7-7.6	22-137	234-920	330-1290	100-400	17-389	2-41.6	31-183	17-59
		Mean	6.57	71	404	542	319	93	7	99	35
		SD	0.6	43	183	236	50	107	11	34	13
TSR	(N=1) (n=11)	Min-Max	7.8-8.8	130-144	894-1290	1142-1740	200-450	134-210	1.3-12	46-71	56-148
		Mean	8.2	137	1153	1502	368	166	5.2	58	89
		SD	0.3	33	261	170	68	25	3	8	25

*ESR=Eastern salt range, *CSR=Central salt range *TSR=Trans-Indus salt range, *N=no. of sampling sites, *n=sampling wells, *SD standard deviation

Supplementary Information
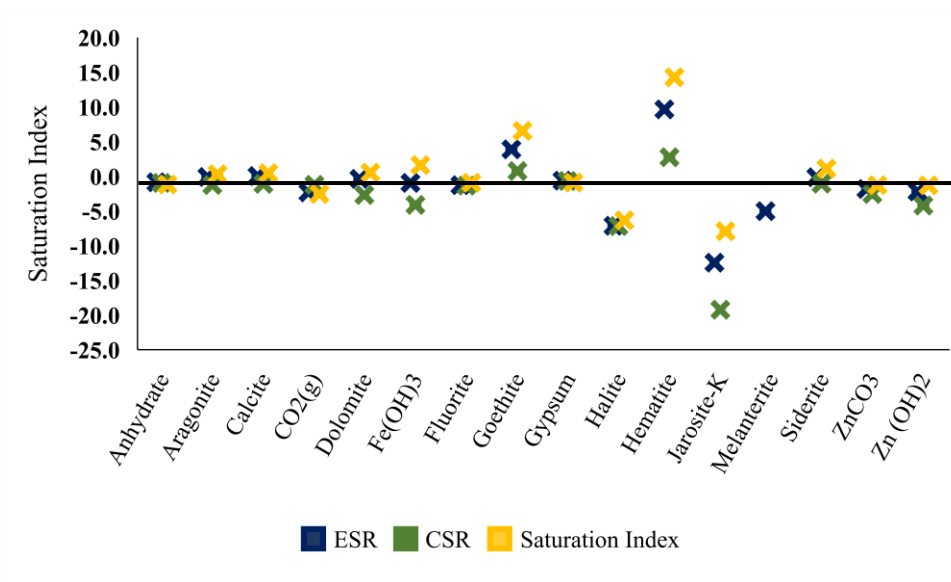
Online Source 1. Geochemical modelling results for saturation indices (SI) for selected minerals in the groundwater water samples. Values of SI > 0 (horizontal line) suggest supersaturation, and values of SI < 0 suggest undersaturation with respect to each mineral.
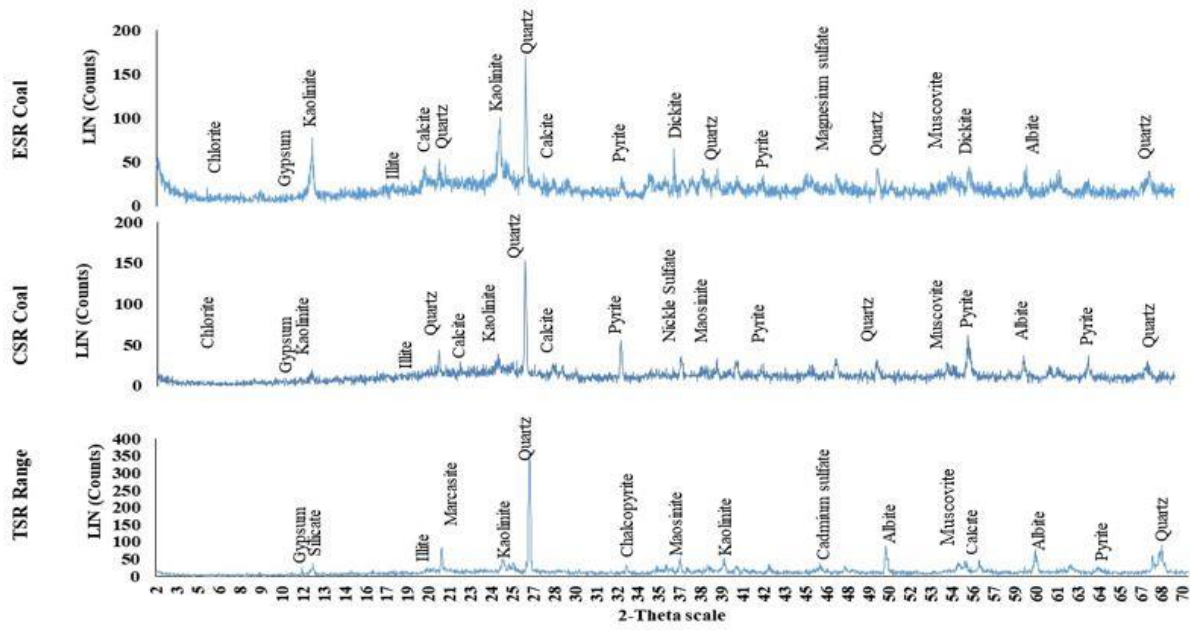
Online Source 2. XRD patterns of coal samples of ESR-Eastern Salt Range, CSR- Central Salt Range, and TSR-Trans-Indus Salt Range.

Online Sounrce 3(a): Correlation matrices of groundwater contaminants in the ESR site.

	Depth	pH	EC	TDS	HCO₃⁻	SO₄²⁻	NO₃⁻	Cl⁻	F⁻	Na⁺	K⁺	Ca²⁺	Mg²⁺
Depth	1	-0.1	0.1	0.1	-0.1	-.3**	0.1	0.1	0.2	0.1	0.1	0.1	-0.2
pH		1	0	0	0.1	-0.1	-.2*	0.2	0.3	-0.1	-0.1	-.3*	.4**
EC			1	.9**	.2*	.4**	.3**	-0.2	-0.3	0	.4**	.2*	.2*
TDS				1	.2*	.4**	.3**	-0.1	-0.3	0	.4**	.2*	.2*
HCO₃⁻					1	.4**	-0.1	-.6**	0.3	0	0.2	-0.1	.3**
SO₄²⁻						1	0.2	-.6**	0.2	0.1	.2*	-0.1	.2*
NO₃⁻							1	-.2*	0.3	0.1	.4**	0.2	0
Cl⁻								1	-0.4	0.1	-0.1	.3**	0.2
F⁻									1	0.3	-0.1	-0.3	0
Na⁺										1	-0.1	0.1	-0.1
K⁺											1	.3**	0
Ca²⁺												1	-.4**
Mg²⁺													1

** Correlation is significant at the 0.01 level (1-tailed).
* correlation is significant at the 0.05 level (1-tailed).

Online Source 3(b): Correlation matrices of groundwater contaminants in the CSR site.

	Depth	pH	EC	TDS	HCO₃⁻	SO₄²⁻	NO₃⁻	Cl⁻	F⁻	Na⁺	K⁺	Ca²⁺	Mg²⁺
Depth	1	.5**	-.4*	-.4*	-0.3	0	0	-.4*	0.2	-.4*	-0.3	0.3	-0.1
pH		1	-0.2	-0.2	0	-0.1	0.2	-0.1	-0.2	-0.1	-0.1	0.2	-0.2
EC			1	.9**	0.2	0.3	.4*	.9**	-0.1	.9**	.9**	0	.5*
TDS				1	0.2	.4*	.4*	.9**	-0.1	.9**	.9**	0	.5*
HCO₃⁻					1	-.4*	.5**	0.3	-0.4	0.2	0.2	-0.3	-0.2
SO₄²⁻						1	0.3	0.1	.7*	0.3	0.1	.4*	.8**
NO₃⁻							1	.4*	0.3	0.3	.4*	.5*	0.3
Cl⁻								1	-0.3	.9**	.9**	-0.1	0.2
F⁻									1	0.1	-0.4	-0.3	.8**
Na⁺										1	.8**	-0.2	0.3
K⁺											1	0.05	0.3
Ca²⁺												1	.5*
Mg²⁺													1

** Correlation is significant at the 0.01 level (1-tailed).
* correlation is significant at the 0.05 level (1-tailed).

Online Source 3(c): Correlation matrices of groundwater contaminants in the TSR site.

	Depth	pH	EC	TDS	HCO$_3$-	SO$_4$$^{2-}$	NO$_3$-	Cl-	F-	Na$^+$	K$^+$	Ca^{2+}	Mg^{2+}
Depth	1	0	0.4	0.3	-.5*	0.2	-.7**	-0.4	0.5*	-0.3	-0.3	0.3	-0.5
pH		1	6.*	.7*	-0.3	0.3	0.2	0	0.8*	0.3	0.3	-0.5	0.3
EC			1	.8**	0	-0.1	0.2	0.3	0.3	0.3	-0.4	0	0.2
TDS				1	-0.3	0.5*	0.2	0	0.8*	0.4	0.2	-0.1	0.1
HCO$_3$-					1	-.5*	0.4	.7*	-0.4	0.5	-0.2	0.2	0.5
SO$_4$$^{2-}$						1	0.4	-.7*	0.8*	0.2	.6*	-0.1	-0.3
NO$_3$-							1	.6*	0.3	0.4	0.4	-0.3	.8**
Cl-								1	-0.2	0.3	-0.3	0.1	.8**
F-									1	0.2	0.7	-0.6	0.3
Na$^+$										1	0.3	0.3	0.4
K$^+$											1	-0.3	0.2
Ca^{2+}												1	-0.3
Mg^{2+}													1

** Correlation is significant at the 0.01 level (1-tailed).
* correlation is significant at the 0.05 level (1-tailed).